

# Lagrangian structure functions in fully-developed hydrodynamical turbulence

K.P. Zybin\*, V.A. Sirota, A.S. Ilyin, A.V. Gurevich

P.N.Lebedev Physical Institute, Russian Academy of Sciences, Moscow, Russia

## Abstract

The Lagrangian velocity structure functions in the inertial range of fully developed fluid turbulence are derived basing on the Navier-Stokes equations. For time  $\tau$  much smaller than the correlation time, the structure functions are shown to obey the scaling relations  $K_n(\tau) \propto \tau^{\zeta_n}$ . The scaling exponents  $\zeta_n$  are calculated analytically. The obtained values are in amazing agreement with the unique experimental results of the Bodenschatz group [1]. New notion – the Lagrangian position structure functions  $R_n(\tau)$  is introduced. All the  $R_n$  of the order  $n > 3$  are shown to have a universal scaling.

## 1 Introduction

The spectrum of velocity pulsations in a turbulent flow can be naturally divided into three ranges: the large scales, the inertial range, and the viscous range. The largest scales  $L$  are comparable with the size of the turbulent volume. These are, roughly speaking, the scales of the largest vortices generated in the flow. The large-scale turbulence is a direct result of laminar flow instability for given boundary conditions. It is always non-uniform and anisotropic, the amplitudes of velocity pulsations are the largest at these scales. The most part of turbulent energy is contained in the large scales. On the other hand, viscous effects play a dominant role at scales smaller than the Kolmogorov scale  $\eta = L/R^{3/4}$ , where  $R$  is the Reynolds number [2]. As the viscosity decreases, the dissipative range becomes narrower. The intermediate range of scales  $\eta \ll \lambda \ll L$  is called the inertial range. In these scales, there is no energy dissipation; the energy flows in Fourier space from large scales to the viscous range. Since viscosity is negligible in the inertial range, the Navier-Stokes equation can be reduced to the incompressible Euler limit [3].

---

\*E-mail: zybin@lpi.ru

Hereafter we discuss the inertial range of locally homogeneous, locally isotropic, statistically stationary turbulent flow of incompressible liquid. The phenomenological theory of such turbulence constructed by Kolmogorov (K41 theory) predicts universal scaling laws for all statistical values. However, experiments have revealed departure from K41 caused by intermittency.

In [4] we proposed a new model of turbulence explaining the intermittency and built on the Navier-Stokes Equation. Our idea was that the main role in statistics (in particular, in structure functions) belongs to the regions with very high vorticity. We showed that these regions stretch out taking the form of vortex filaments. We also showed that the growth of vorticity in the filaments is caused by large-scale pulsations. A considerable simplification of the problem is reached by treating the fully developed turbulence from Lagrangian viewpoint, which is natural from theoretical point of view [5]. We obtained the equation for the probability distribution function (PDF) of vorticity, and time dependence of its statistical moments. Note that recently the model equation interpreting the experimental data have been proposed [6]. This model is phenomenological and is not based on the Navier-Stokes Equation.

This paper is a continuation of [4]. We apply the theory developed in [4] to obtain the Lagrangian statistical moments of velocity differences also called the Lagrangian structure functions

$$K_n(\tau) = \langle |\mathbf{v}(t + \tau) - \mathbf{v}(t)|^n \rangle , \quad (1)$$

where the values of velocity are taken along the trajectory of a liquid particle, and the angle brackets denote the average over the ensemble of trajectories. We find a relation connecting the Lagrangian structure functions of different orders. It may be used as an analogue to the extended self-similarity ansatz (established for the Euler case) [7, 1] in the Lagrangian case.

Recently there has been a significant experimental progress in measuring the Lagrangian statistical properties [1, 8]. We compare the predictions of our theory with recent experimental results of the Bodenschatz group [1] and find a wonderful agreement.

The paper is organized as follows. In §2, we recall briefly the method and some of the results obtained in [4]. In particular, we derive the time dependence of statistical moments of vorticity in a vortex filament. In §3, basing on these results, we calculate the scaling exponents of the Lagrangian velocity structure functions (1). We also derive a relation between the structure functions of different orders, which may be valid even in the cases when there is no scaling (for example, near to the boundaries of the inertial interval). In §4, the theoretical results are compared with the experimental data. In §5, we introduce a new notion: Lagrangian structure functions of position. We calculate their scaling exponents on the basis of our model. These results can also be checked by experiments.

## 2 Properties of turbulent structures in the inertial interval.

We consider the Navier-Stokes equation for incompressible liquid. At the scales inside the inertial range the equation takes the form of the Euler equation:

$$\frac{\partial \mathbf{v}}{\partial t} + (\mathbf{v} \cdot \nabla) \mathbf{v} + \frac{\nabla p}{\rho} = 0, \quad \nabla \cdot \mathbf{v} = 0, \quad (2)$$

where  $\mathbf{v}$  is the velocity of the flow and  $p$  is the pressure. The density  $\rho$  is taken to be unity below. The second equation expresses the incompressibility of the liquid. The restriction of scales by the inertial range presumes, in particular, that we consider only smooth initial conditions. The equation for pressure follows from (2):

$$-\Delta p = \nabla_i v_j \cdot \nabla_j v_i \quad (3)$$

Thus, the equations system (2) is complete. We note that (2) can be rewritten as

$$\frac{\partial \boldsymbol{\omega}}{\partial t} = \text{rot} [\mathbf{v}, \boldsymbol{\omega}],$$

where  $\boldsymbol{\omega} = \text{rot } \mathbf{v}$  is vorticity.

We now discuss the formation of stretched structures – vortex filaments – in the turbulent flow. They appear as a result of flow instability caused by large-scale pressure pulsations [4]. Random large-scale forces stretch a liquid drop forming a filament. The main role in the process belongs to the incompressibility of the liquid. First, the volume conservation results in transversal compression of the filament during its straining. Conservation of angular momentum then leads to acceleration of rotating and hence to growth of vorticity in the filament. Second, the sound speed in an incompressible liquid is infinite. This means an instant transport of large-scale pressure pulsations, which cause the stretching of the filaments.

To illustrate these statements, we consider an axially symmetric flow. The hydrodynamic equations for the radial, azimuthal, and axial velocity components  $v_r$ ,  $v_\phi$ , and  $v_z$  are

$$\begin{aligned} \frac{\partial v_r}{\partial t} + v_r \frac{\partial v_r}{\partial r} + v_z \frac{\partial v_r}{\partial z} - \frac{v_\phi^2}{r} &= -\frac{\partial p}{\partial r} \\ \frac{\partial v_\phi}{\partial t} + v_r \frac{\partial v_\phi}{\partial r} + v_z \frac{\partial v_\phi}{\partial z} + \frac{v_\phi v_r}{r} &= 0 \\ \frac{\partial v_z}{\partial t} + v_r \frac{\partial v_z}{\partial r} + v_z \frac{\partial v_z}{\partial z} &= -\frac{\partial p}{\partial z} \end{aligned} \quad (4)$$

$$\frac{1}{r} \frac{\partial}{\partial r} (r v_r) + \frac{\partial v_z}{\partial z} = 0 \quad (5)$$

We seek a solution of the system (4), (5) in the linear form

$$v_\phi = \omega(t)r, \quad v_r = a(t)r, \quad v_z = b(t)z \quad (6)$$

The corresponding pressure following from (6) must be

$$p(r, z, t) = \frac{P_1(t)}{2}r^2 + \frac{P_2(t)}{2}z^2$$

The equation (5) then implies a relation between  $a$  and  $b$ :

$$2a + b = 0. \quad (7)$$

This means the fluid volume conservation. Indeed, we consider a cylindrical drop with a radius  $R(t)$  and a length  $Z(t)$  at an instant  $t$ . Then it follows from (6) that

$$\dot{R} = a(t)R, \quad \dot{Z} = b(t)Z,$$

Integrating these equations, we make sure that the cylinder volume conserves:

$$\pi R(t)^2 Z(t) = \pi R_0^2 Z_0 \exp \int_0^t (2a(t_1) + b(t_1)) dt_1 = \pi R_0^2 Z_0.$$

Combining (6) with (4), we obtain a system of ordinary differential equations:

$$\begin{aligned} \dot{a} + a^2 - \omega^2 &= -P_1 \\ \dot{\omega} + 2a\omega &= 0 \\ \dot{b} + b^2 &= -P_2 \end{aligned} \quad (8)$$

Differentiating the second equation of system (8) and substituting other equations, we obtain

$$\ddot{\omega} = -P_2(t)\omega \quad (9)$$

The function  $P_2(t)$  has a meaning of pressure fall along the cylinder axis. Let us suppose that it is determined by large-scale pressure pulsations in turbulent flow. Hence, it is a complicated function of time; we assume that its time average is zero. Then the time intervals when  $P_2(t) > 0$  and  $P_2(t) < 0$  are equally probable. However, at  $P_2(t) > 0$  the function  $\omega(t)$  oscillates, the oscillation amplitude changing weakly. On the contrary, at  $P_2(t) < 0$ , the function  $\omega(t)$  grows exponentially. It is clear that the value of  $\omega$  grows on average. We note also that from (8) and (7) follows the proportionality of  $\omega$  to the cylinder length  $Z$ . Hence, such growth of  $\omega$  means stretching the cylinder. We also note that, despite the nonlinearity of the initial system (4), (5), the final equation (9) is linear. The nonlinearity acts only in the directions transversal to the cylinder axis.

This example illustrates the behavior of a drop with large vorticity in a turbulent flow: it stretches out forming a filament, and the vorticity continues to increase. In [4] we have

analyzed the general equations (2) in terms of Lagrangian variables. We have shown that the development of filaments occurs in a way analogous to that in the considered example. We have found a linear equation analogous to (9) describing the growth of vorticity in the accompanying reference frame:

$$\ddot{x}_n = -\rho_{nk}x_k, \quad x_i = \omega_i, \quad \rho_{nk} = \nabla_n \nabla_k P \quad (10)$$

Here  $x_i$  and  $P$  are the components of  $\boldsymbol{\omega}$  and the pressure in the Lagrangian reference frame. The matrix  $\rho_{nk}$  is generated by large-scale pulsations. In order to obtain the statistical properties of the flow, it must be considered as a random quantity. Hence, (10) is a stochastic equations set.

Instead of three equations of the second order, we consider a set of six first-order equations:

$$\dot{x}_i = y_i \quad \dot{y}_i = -\rho_{ij}x_j \quad (11)$$

We introduce the joint probability density

$$f(t, \mathbf{x}, \mathbf{y}) = \langle \delta(\mathbf{x} - \mathbf{x}(t))\delta(\mathbf{y} - \mathbf{y}(t)) \rangle . \quad (12)$$

Here  $\mathbf{x}(t)$  and  $\mathbf{y}(t)$  are the solutions of (11) at the given realization of  $\rho_{ij}$  and initial conditions; the average is taken over the ensemble of all possible realizations. The variables  $\mathbf{x}$  and  $\mathbf{y}$  are independent.

Let the flow be locally homogeneous and isotropic. Then, assuming statistical independency of different components of the matrix  $\rho_{ij}$ , we obtain from (11) the Fokker-Planck equation for  $f$  (see [4]):

$$\frac{\partial f}{\partial t} + y_k \frac{\partial f}{\partial x_k} = \left[ x^2 \frac{\partial^2 f}{\partial \mathbf{y}^2} + \left( x_k \frac{\partial}{\partial y_k} \right)^2 f \right], \quad (13)$$

where  $t$  is normalized by the characteristic time of the probability density change that is of the order of the correlation time.

For what follows we need an asymptotic time dependence of the moments  $\langle x^{2n} \rangle$ . To find it we consider the invariant moments of the even order  $2P$ :

$$M_P(n, m, k) = \langle x^{2n} y^{2m} (\mathbf{xy})^k \rangle \equiv \int x^{2n} y^{2m} (\mathbf{xy})^k f d\mathbf{x}d\mathbf{y}, \quad n + m + k = P$$

Integrating (13) with appropriate weights, we obtain for these moments a closed set of linear differential equations

$$\begin{aligned} \frac{d}{dt} M_P(n, m, k) = & 2n M_P(n-1, m, k+1) + 2m(4k+2m+2) M_P(n+1, m-1, k) \\ & + 4m(m-1) M_P(n, m-2, k+2) + k M_P(n, m+1, k-1) + 2k(k-1) M_P(n+2, m, k-2) \end{aligned}$$

The number  $Q$  of equations in the set is equal to a number of combinations  $(n, m, k)$  such that  $n + m + k = P$ :

$$Q = \frac{1}{2}(P + 1)(P + 2)$$

Thus, the evolution of the  $2P$ -order invariant moments is described by the set of  $Q$  linear differential equations. As  $t \rightarrow \infty$ , the solutions increase exponentially, in particular  $\langle x^{2n} \rangle \propto \exp(\Lambda_{2n}t)$ ,  $\Lambda_{2n}$  being the maximal root of the corresponding characteristic equation. Since  $\langle x^{2n} \rangle$  is positive, the solution must not oscillate, and the root must be real. To find the exponents, we calculate the determinants and solve the characteristic (algebraic) equations numerically. The first sixteen values  $\Lambda_n$  are

$$\begin{aligned} \Lambda_2 &= 2.52, & \Lambda_4 &= 6.12, & \Lambda_6 &= 10.43, & \Lambda_8 &= 15.25, \\ \Lambda_{10} &= 20.48, & \Lambda_{12} &= 26, & \Lambda_{14} &= 32.03, & \Lambda_{16} &= 38.25 \\ \Lambda_{18} &= 44.73, & \Lambda_{20} &= 51.46, & \Lambda_{22} &= 58.42, & \Lambda_{24} &= 65.58 \\ \Lambda_{26} &= 72.95, & \Lambda_{28} &= 80.52, & \Lambda_{30} &= 88.26 & \Lambda_{32} &= 96.16 \end{aligned} \tag{14}$$

To summarize, we cite [4] to list the main properties of the equation (13) concerning the moments:

1. All  $n$ -order moments of  $x_k$  and  $y_j$  are connected by a set of first-order linear differential equations. Hence, it is possible to evaluate the moments of any order.
2. The even moments grow exponentially. Independently of the initial conditions, the function  $f$  at large values of  $t$  depends only on the moduli  $x$  and  $y$  and on the cosine of the angle between the vectors  $\mu = (\mathbf{x}, \mathbf{y})/xy$ .
3. The higher even moments grow faster than the lower ones.

The properties 2 and 3 express the presence of intermittency. For example, for large values of  $t$  we have  $\langle x^{2n} \rangle \gg \langle x^2 \rangle^n$ .

### 3 Lagrangian structure functions

As shown in Section 2, regions of large vorticity in a turbulent flow take the form of filaments stretched along the vorticity direction.

Then a typical trajectory in the flow demonstrates two types of behavior shown in Fig. 1. In the region I the vorticity is not very large, and the trajectory is smooth, the characteristic time of velocity change is of the order of the correlation time  $\tau_c$ . In the region II the vorticity is large, the test particle oscillates with frequency  $\omega$ . These second regions give the main contribution to correlation functions. Indeed, the second order Lagrangian structure function  $K_2(\tau)$  is proportional to  $\tau^2$  in "smooth" parts of trajectory, and we shall see below that in the "oscillating" parts it is proportional to  $\tau$ .

So, we consider the regions with large  $\omega$ . We choose a cylindric frame with the origin in the local maximum of  $\omega$ , the axis  $z$  directed along  $\omega$ . Since there is fast rotation around

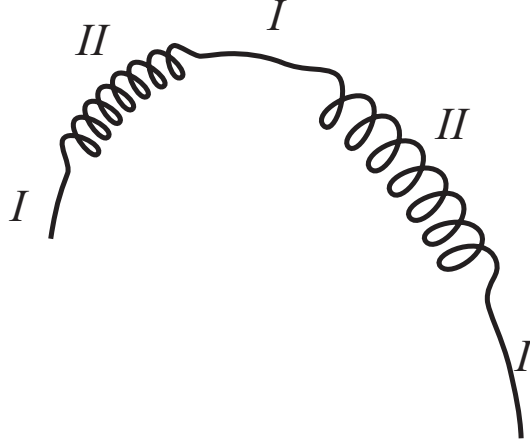


Fig.1. A typical trajectory of a test particle.

the  $z$  axis near the origin, the flow does not depend on the angle  $\phi$ . Then in the linear approximation we obtain the expression (6) which returns us to the example considered in Section 1:

$$v_\phi = \omega(t)r, \quad v_r = a(t)r, \quad v_z = b(t)z \quad (15)$$

Conservation laws for mass and for angular momentum along the  $z$  axis take the form (see (7), (8))

$$2a + b = 0,$$

$$\dot{\omega} = -2a(t)\omega$$

From (15) we find

$$\frac{dr}{dt} = a(t)r, \quad \frac{dz}{dt} = b(t)z, \quad \frac{d\phi}{dt} = \omega(t) \quad (16)$$

The parameters  $\omega, a, b$  change slowly, with characteristic time  $\tau_c$ . To the contrary, the oscillations are fast,  $\omega\tau_c \gg 1$ . Hence, with accuracy  $\tau/\tau_c$  we have

$$|\delta\mathbf{v}| = |\mathbf{v}(t + \tau) - \mathbf{v}(t)| = 2v_\phi \sin \frac{\delta\phi}{2} = 2r\omega \sin \frac{\omega\tau}{2} \quad (17)$$

To calculate the correlation functions of degree  $n$  we must raise an absolute value of  $\delta\mathbf{v}$  to the  $n$ -th power and take an ensemble average with the probability distribution function.

We first consider the pair correlation function

$$K_2(\tau) = \langle (v(t + \tau) - v(t))^2 \rangle$$

In accordance with the above, it has the form

$$K_2(\tau) \propto \int P(\omega, t) \omega^2 \sin^2(\omega\tau/2) d\omega \quad (18)$$

In [4] we have analyzed the solution of (13) and the integrated PDF  $P(x) = \int f(x, y, \mu) x^2 d\mathbf{y} d\mu$  (here  $\mu$  is the cosine of the angle between  $\mathbf{x}$  and  $\mathbf{y}$ ). We have found that  $P(\omega)$  has an intermediate stationary asymptote

$$P(\omega) = C\omega^{-4} \quad (19)$$

For small and for infinitely large values  $\omega$ , the PDF remains non-stationary.

We see that the integral (18) converges for the stationary PDF (19). Actually,

$$K_2(\tau) \propto \int_0^\infty \frac{\omega^2 \sin^2(\omega\tau/2)}{\omega^4} d\omega \propto \tau \int_0^\infty \frac{\sin^2(q)}{q^2} dq$$

(The input of  $\delta v_z^2$  is small – proportional to  $z^2$ ).

So, for  $\tau \ll \tau_c$  the second order structure function along the Lagrangian trajectory is

$$K_2(\tau) \propto \tau \quad (20)$$

This result adjusts with the Kolmogorov's theory K41 [2],[3].

For higher-order structure functions  $K_n(\tau)$  we have

$$K_n(\tau) \propto \int_0^\infty P(\omega, t) \omega^n |\sin(\omega\tau/2)|^n d\omega \quad (21)$$

The integral with the stationary PDF diverges. Hence, the higher structure functions are determined by the non-stationary part of the PDF. To calculate  $K_n(\tau)$ , we use the moments

$$\int_0^\infty P(\omega, t) \omega^{2n} d\omega \propto e^{\Lambda_{2n} t}$$

found in Section 2. We expand the sine in (21) into the series and integrate each term. For time  $t$  satisfying

$$1 \ll t \ll \frac{\ln(\tau^{-2})}{\Lambda_{2n+2} - \Lambda_{2n}}, \quad \tau \rightarrow 0$$

the second item is much less than the first one. We restrict ourselves by the first term as  $\tau \rightarrow 0$ . Then

$$K_n(\tau) \propto \tau^n e^{\Lambda_{2n} t} \quad (22)$$

Excluding  $t$ , we obtain

$$\left( \frac{K_m(\tau)}{\tau^m} \right)^{1/\Lambda_{2m}} = \left( \frac{C_{n|m} K_n(\tau)}{\tau^n} \right)^{1/\Lambda_{2n}} \quad (23)$$

Here  $C_{n|m}$  are constants not depending on  $\tau$ . This relation connects the structure functions of different orders. Choosing  $m = 2$  and taking (20) into account, we find

$$K_n \propto \tau^{\zeta_n},$$

where

$$\zeta_n = n - \frac{\Lambda_{2n}}{\Lambda_4} \quad (24)$$

Using (14) we get first twelve scaling exponents  $\zeta_n$ :

$$\begin{aligned} \zeta_1 &= 0.59, & \zeta_2 &= 1, & \zeta_3 &= 1.3, & \zeta_4 &= 1.51, \\ \zeta_5 &= 1.65, & \zeta_6 &= 1.75, & \zeta_7 &= 1.77, & \zeta_8 &= 1.75, \\ \zeta_9 &= 1.69, & \zeta_{10} &= 1.59, & \zeta_{11} &= 1.45, & \zeta_{12} &= 1.28 \end{aligned}$$

Actually, the stationary structure function (20) is not necessary to determine the scaling exponents. The reason is that the parameters  $\Lambda_{2n}$  grow fast as a function of  $n$ . For example, we take  $m = 16$ . Using (23) with  $\Lambda_{32} = 96.16$ , we then obtain

$$K_n(\tau) \propto \tau^{n-16\Lambda_{2n}/\Lambda_{32}} K_{16}^{\Lambda_{2n}/\Lambda_{32}}$$

For small  $n$  the ratio  $\Lambda_{2n}/\Lambda_{32}$  is small enough, and we can put  $K_{16}^{\Lambda_{2n}/\Lambda_{32}} \approx 1$ . For  $n = 2$  we then find  $K_2(\tau) \propto \tau^{0.98} \approx \tau$ . The result is very close to that obtained with the stationary PDF. We note that this relation is derived now from (23) only. This demonstrates the consistency between the stationary and non-stationary solutions of the equation (13). Taking other values of  $n$ , we get in the same way

$$\begin{aligned} \zeta'_1 &= 0.58, & \zeta'_2 &= 0.98, & \zeta'_3 &= 1.26 \\ \zeta'_4 &= 1.46, & \zeta'_5 &= 1.59, & \zeta'_6 &= 1.67 \end{aligned}$$

We recall that in the derivation of (23) we neglected the rest of the sine expansion in (21) as  $\tau \rightarrow 0$ . To justify this approximation, we calculate (21) with complete sine expansion, using the moments of  $\omega$ . We then express  $e^t$  through  $K_{16}$  using (22). For example, for  $K_2$  we have

$$\begin{aligned} K_2 &= \frac{1}{4}\tau^2 e^{\Lambda_4 t} - \frac{1}{48}\tau^4 e^{\Lambda_6 t} + \frac{1}{1440}\tau^6 e^{\Lambda_8 t} + \dots \\ &= \frac{1}{4}\tau^{0.98} K_{16}^{0.06} - \frac{1}{48}\tau^{2.26} K_{16}^{0.11} + \frac{1}{1440}\tau^{3.46} K_{16}^{0.16} + \dots \end{aligned} \quad (25)$$

We see that as  $\tau \rightarrow 0$  the series converges rapidly, and the rest is small with respect to the first term. The same is correct for the structure functions of higher orders.

We note also that the relation (23) can be rewritten as

$$C_{n|m} = \frac{K_m^{\Lambda_{2n}/\Lambda_{2m}}}{K_n} \tau^{n-m\frac{\Lambda_{2n}}{\Lambda_{2m}}} \quad (26)$$

According to our theory, these combinations of structure functions must be constant, i.e. they must not depend on  $\tau$ .

## 4 Comparison of the theory with the experiment.

In this Section we compare the predictions of our theory with the results of recent experiments of the Bodenschatz group [8],[1]. In these experiments turbulence was generated by two counter-rotating disks. Different regimes of the facility allowed to make the measurements for different local Reynolds numbers  $R_\lambda$ . The Lagrangian test particles used to trace the flow had the size comparable or smaller than the Kolmogorov scale  $\eta$  for all tested Reynolds numbers. The motion of particles was tracked in a subvolume of about  $10^{-4}$  of the whole turbulent volume, in the center of the tank where the effects of the mean velocity were negligible. Thus, this region seems to us optimal for investigation of locally homogenous turbulence.

The measurements performed in [8] showed directly the presence of stretched structures – vortex filaments. It was shown that near to these structures the absolute values of particle accelerations were maximal. The probability distribution of these accelerations was found to be significantly non-gaussian in the region of their large values. Thus, general picture of vortex structures in turbulence corresponds to that in our theory [4].

Table 1. Values of the scaling exponents normalized by  $\zeta_2$ . The experimental results for different local Reynolds numbers are cited from [1]

$R$	200	690	815	Theory
$\zeta_1/\zeta_2$	$0.59 \pm 0.02$	$0.58 \pm 0.05$	$0.58 \pm 0.12$	0.59
$\zeta_3/\zeta_2$	$1.24 \pm 0.03$	$1.28 \pm 0.14$	$1.28 \pm 0.30$	1.3
$\zeta_4/\zeta_2$	$1.35 \pm 0.04$	$1.47 \pm 0.18$	$1.47 \pm 0.38$	1.51
$\zeta_5/\zeta_2$	$1.39 \pm 0.07$	$1.61 \pm 0.21$	$1.59 \pm 0.46$	1.65
$\zeta_6/\zeta_2$	$1.40 \pm 0.08$	$1.73 \pm 0.25$	$1.66 \pm 0.53$	1.75
$\zeta_7/\zeta_2$	$1.39 \pm 0.09$	$1.83 \pm 0.28$	$1.67 \pm 0.60$	1.77
$\zeta_8/\zeta_2$	$1.40 \pm 0.10$	$1.92 \pm 0.32$	$1.65 \pm 0.66$	1.75
$\zeta_9/\zeta_2$	$1.42 \pm 0.11$	$1.97 \pm 0.35$	$1.61 \pm 0.73$	1.69
$\zeta_{10}/\zeta_2$	$1.46 \pm 0.12$	$1.98 \pm 0.38$	$1.57 \pm 0.80$	1.59

We make the quantitative comparison of the Lagrangian structure functions obtained in our theory with the results of the experiment [1]. Table 1 and Fig. 2 show the Lagrangian scaling exponents  $\zeta_n$  normalized by  $\zeta_2$ , up to the 10th order. The first three columns of Table 1 represent the values measured in [1] with different local Reynolds numbers  $R_\lambda$ . The last column contains our theory prediction (24). The theory is in excellent agreement with the experimental data. Moreover, the agreement is better for larger values of  $R_\lambda$ . This corresponds to the fact that the theory is constructed in the limit  $R \rightarrow \infty$ . Also, both in the theory and in the experiment with the most value of  $R_\lambda$ , the scaling exponents grow

up to the 7-th order, and then decrease. We note that the theory predicts also the scaling exponents of higher orders that are not measured yet.

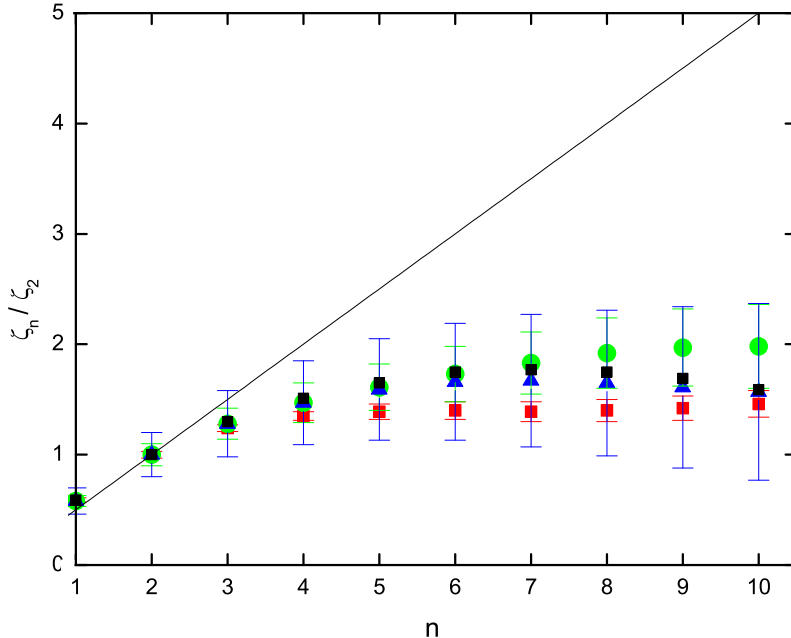


Fig.2 Scaling exponents  $\zeta_n$  normalized by  $\zeta_2$  as a function of order. Small black squares denote the prediction of our theory, other symbols show the experimental results [1] for different local Reynolds numbers:  $R_\lambda = 200$  (red squares),  $R_\lambda = 690$  (green circles), and  $R_\lambda = 815$  (blue triangles). The solid line corresponds to the Kolmogorov theory K41. Strong departure from the K41 prediction of both the experiment [1] and our theory is the manifestation of intermittency.

Table 1 and Fig. 2 also demonstrate the growth of dispersion of the measured scaling exponents as a function of order and of  $R_\lambda$ . This is in accord with the presented theory, which is based on the notion that filaments (narrow regions with very high vorticity) make the most contribution to structure functions. The dispersion behavior is then the result of intermittency. The higher is the order, the more important become very high peaks, the more seldom they occur. Hence, for a given sample the dispersion increases with the moment order. On the other hand, the real height of peaks is limited by viscosity.<sup>1</sup> As viscosity decreases, the size of a sample needed to determine the statistical moments increases. This property of statistical systems is demonstrated, in particular, in [9].

<sup>1</sup>Presumably, the viscosity constrains the value of  $m$  in (23). We choose  $m = 16$  as an upper limit because the ratio of the large-scale characteristic time  $\tau_c$  to the viscous Kolmogorov time  $\tau_\eta$  is about 100. Since the time of change of  $K_{16}$  is  $\Lambda_{32}^{-1} \approx 0.01\tau_c$ , it lies near the boundary between the inertial and the viscous ranges.

In addition to analysis of the scaling exponents, we also compare (23) with direct experimental data [1] for dependence of the high-order Lagrangian structure functions of  $\tau$ . For that we choose the form (26) of the equation (23) to check if the combinations  $C_{n|m}$  of any two structure functions are constant. The results for  $C_{10|9}$  and  $C_{10|8}$  are presented in Fig.3. We see that even for the highest of the measured orders, the values  $C$  are constant up to the accuracy of the available experimental graph.

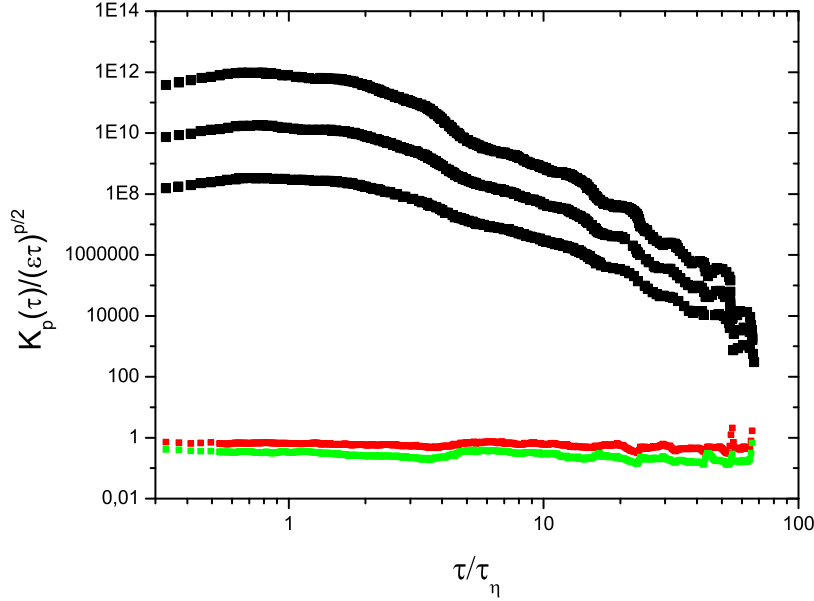


Fig.3. Lagrangian structure functions of the orders 8,9, 10 (black curves from the bottom to the top) normalized by the K41 predictions ( $R_\lambda = 690$ ): cited from [1]. Red and green curves denote the functions  $C_{10|9}$  and  $C_{10|8}$ , respectively.

We stress that no adjustable parameters were used in calculating both the scaling exponents (Table 1, Fig.2) and the combination of the Lagrangian structure functions (Fig.3). Thus, the coincidence between the theoretical predictions and the experimental results is wonderful. One can suppose that a significant role belongs to a happy choice of parameters of the experiment: very homogeneous flow in the subvolume where the measurements were performed, and the size of test particles coinciding with the Kolmogorov scale. Due to this the high frequency noise is damped in the measurements, and the experimental data describe the inertial range only. Exactly this range is studied by the theory.

## 5 Universal scaling for Lagrangian structure functions of position.

The Lagrangian approach gives a possibility to study not only the statistical properties of velocities, but also that of positions of the particles. This allows to introduce a new notion in the turbulence theory. Define the Lagrangian structure functions of positions of two particles as

$$R_n(\tau) = \langle |\mathbf{r}(t + \tau) - \mathbf{r}(t)|^n \rangle$$

As in the case of velocity structure functions, the main contribution in  $R_n$  comes from the regions with large vorticity. Integrating (16) and calculating  $|\delta\mathbf{r}|$  by analogy with (17), we obtain

$$R_n(\tau) \propto \int P(\omega) \sin^n(\omega\tau/2) d\omega \propto \int \frac{\sin^n(\omega\tau/2)}{\omega^4} d\omega$$

If  $n > 3$  the integral with the stationary PDF (19) converges. Hence, the high-order structure functions of positions are determined by the stationary part of the PDF. We note that in the asymptotics all the scaling exponents are equal:

$$R_n(\tau) \propto \int \frac{\sin^n(\omega\tau/2)}{\omega^4} d\omega \propto \tau^3, \quad n > 3$$

In other words, there is a universal scaling for all  $R_n$ ,  $n > 3$ . This universal scaling, if it would be observed in experiments, can be an evidence for the determining influence of the filaments on the behavior of the structure functions in the inertial range.

## 6 Conclusion

To conclude, we list the main results of the paper.

1. The Lagrangian velocity structure functions of high orders are derived in the inertial interval of fully developed liquid turbulence.
2. The comparison of the theory predictions with experimental results shows an excellent agreement.
3. New experimentally measurable values – the Lagrangian position structure functions are introduced and calculated. Their scaling exponents are shown to be independent on the order of the function for any  $n > 3$ .

We emphasize that no adjustable parameters were used for the scaling exponents. Also the power-law dependence of the Lagrangian structure functions was not suggested in the model. All the obtained relations are the consequences of the equation (13) derived directly from the Navier-Stokes equation in the inertial interval.

## References

- [1] H.Xu, M.Bourgoin, N.T.Ouellette, E.Bodenschatz, Phys.Rev.Lett **96**, 024503, (2006)
- [2] L.D. Landau, E.M. Lifchitz, 'Hydrodynamics', Moscow, Nauka, 1986
- [3] U.Frisch, 'Turbulence. The legacy of A.N. Kolmogorov', Cambridge Univ. Press, 1995
- [4] K.P. Zybin, V.A. Sirota, A.S. Il'in, A.V. Gurevich, JETP 2007, Vol.105, N 2, p. 455 ,  
arXiv:physics/0612131
- [5] P.K. Yeung Annu.Rev.Fluid Mech. **34**, 115 (2002)
- [6] C. Beck, Phys.Rev.Lett. **98**, 064502 (2007)
- [7] R. Benzi, S. Ciliberto, R. Tripiccone, C. Baudet, F. Massaioli, and S. Succi, Phys. Rev. E **48**, R29 (1993)
- [8] G.A.Voth, A.La Porta, A.M.Grawford, J.Alexander, E.Bodenschatz "Measurement of particle accelerations in fully developed turbulence" arXiv:physics/0110027v2 3 Dec 2001
- [9] M.E. Artushkova, D.D. Sokolov, Astronomy Reports **49**, N7, 520 (2005)